Received: 16 November 2020 | Revised: 24 August 2021 | Accepted: 24 August 2021

DOI: 10.1002/ddr.21878

RESEARCH ARTICLE

DRUG DEVELOPMENT RESEARCH WILEY

Astragaloside IV enhances the sensibility of lung adenocarcinoma cells to bevacizumab by inhibiting autophagy

Liang Li | Gao Li | Minbiao Chen | Renzhong Cai

Department of Thoracic Surgery, Hainan General Hospital, Haikou, China

Correspondence
Renzhong Cai, Department of Thoracic Surgery, Hainan General Hospital, No. 19 Xiuhua Road, Haikou, Hainan Province 570311, China.
Email: cairenzhong_crz@163.com

Abstract

Bevacizumab (BV) has an inhibitory effect on tumor growth including lung adenocarcinoma. However, its efficacy is greatly affected by drug resistance. Astragaloside IV (AST-IV) is effective in combination with other drugs is effective to treat cancer. This study aimed to investigate the effect of AST-IV on enhancing the sensibility of lung adenocarcinoma cells to BV. A549 cells were treated by different concentrations of BV and AST-IV. Cell viability, cell cycle, and apoptosis were detected by thiazolyl blue tetrazolium bromide (MTT) and flow cytometry, respectively. Quantitative reverse transcription-polymerase chain reaction (qRT-PCR) and western blotting were performed to detect the expression levels of autophagy- and apoptosis-related proteins, protein kinase B (AKT), and mammalian target of rapamycin (mTOR). The results showed that BV or AST-IV could inhibit the viability and promote the apoptosis of A549 cells in a concentration-dependent manner. Moreover, BV or AST-IV inhibited Bcl-2 expression and increased the expressions of Bax and Cleaved caspase-3, and promoted apoptosis. BV and AST-IV in combination acted synergistically on viability and apoptosis of A549 cells. However, BV alone down-regulated P62 expression, LC3I/LC3II level, the number of cells arrested at S phase and the phosphorylation levels of AKT and mTOR, but upregulated the number of cells arrested at G0/G1 phase and Beclin1 expression, whereas AST-IV alone could reverse the effect of BV on autophagy-related proteins, the phosphorylation levels of AKT and mTOR. This paper demonstrates that AST-IV enhances the effect of BV on inhibiting proliferation and promoting apoptosis of lung adenocarcinoma cells through inhibiting autophagy pathway.

KEYWORDS
apoptosis, astragaloside, autophagy, bevacizumab, proliferation

1 | INTRODUCTION

Lung cancer is a frequent disease threatening human health, which has the highest morbidity and mortality among all malignant tumors (Bade & Dela Cruz, 2020). Lung adenocarcinoma is the main type of lung cancer, accounting for about 80%–85% of all lung cancer cases (Toyokawa et al., 2018). The early clinical symptoms of lung adenocarcinoma are not obvious; however, the disease can rapidly progress to the middle and late stage. Chemotherapy is widely used to treat lung cancer (Ma et al., 2018). Nevertheless, lung adenocarcinoma cells are less sensitive to chemotherapy, thus resulting in poor prognosis of lung adenocarcinoma patients (Chen et al., 2020). Therefore, to further explore the therapies of lung adenocarcinoma has become an urgent practical problem for researchers.

Bevacizumab (BV), a recombinant humanized monoclonal antibody drug against tumor angiogenesis, can inhibit the formation of

tumor blood vessels, which plays an inhibitory role in the growth and metastasis of tumors (Lin et al., 2018; Rossi et al., 2017). Currently, BV is widely used in the treatment of lung cancer (Yang et al., 2017). With the increase resistance to BV, its clinical therapeutic effect is limited (Ramezani et al., 2019; Shan et al., 2019; Tamura et al., 2017). Autophagy process significantly participated in the tumor-suppressive effect of BV on many types of cancer cells (Huang, Song, et al., 2018; Müller-Greven et al., 2017; Wu et al., 2017; Zhao et al., 2018). Autophagy is a common phenomenon in eukaryotic cells and is closely related to the occurrence and development of various diseases (Levy et al., 2017). Autophagy has a bidirectional effect on the growth of tumor. In the early stage of tumor, autophagy can inhibit the growth of tumor cells, and cells will clear out damaged organelles and reduce inflammation under autophagy interference, thus maintaining and protecting intracellular homeostasis and the growth of normal cells (Li et al., 2017). However, in the late stage, autophagy becomes an important factor contributing to the drug resistance of tumor cells, therefore promoting the growth of tumor cells (Li et al., 2017). At present, it is widely accepted that autophagy promotes anti-tumor therapy against tumor such as chemotherapy, while the inhibition of autophagy can increase the sensitivity to anti-tumor treatment in tumor cells (Huang, Wang, & Wang, 2018; Jiang et al., 2018). Hence, autophagy is possibly a potential mechanism by which tumor cell develops resistance to chemotherapy, molecular targeted therapy, and/or other drugs.

Studies have shown that inhibiting cell viability of tumor cells is an important way to control tumor growth, and massive research results have also confirmed that many anti-tumor drugs exert their effects by promoting cell apoptosis (Cao et al., 2017; Meher et al., 2018; Tian et al., 2018). Astragaloside (AST), a main active compound found in *Astragalus membranaceus*, helps promote vasodilation, and improves cardiac energy metabolism, inflammatory, and oxidative conditions (Wang et al., 2020). With the development of anti-tumor studies of traditional Chinese medicine, the anti-tumor effect of AST has attracted increasing research attention. Many studies have demonstrated that AST can inhibit tumor cells proliferation and promote the apoptosis (Xie et al., 2016; Zheng et al., 2018). In addition, astragaloside IV (AST-IV) is the most bioactive type of AST, which has been indicated to enhance the sensitivity of cisplatin in non-small cell lung cancer cells (He et al., 2016). Therefore, AST-IV and BV were used in combination to treat lung adenocarcinoma cell line A549 in this experiment. We explore the effect of the combined application of the two drugs on the proliferation and apoptosis of lung adenocarcinoma cells in vitro and preliminarily investigate the relationships between the combined application of them and autophagy pathways.

2 | MATERIALS AND METHODS

2.1 | Cell culture and cell treatment

Human lung adenocarcinoma cell lines A549 cells were purchased from the Cell Bank of the Chinese Academy of Sciences (Shanghai, China) and were cultured with Roswell Park Memorial Institute (RPMI)-1640 medium (Gibco, United States) containing 10% fetal bovine serum (FBS, Gemini Bio-Products, Sacramento, CA, United States) in an incubation box at 37°C with 5% CO_2. The cells in the logarithmic growth phase were selected for experiments.

A549 cells were divided into control group, BV different concentrations of treatment group, AST-IV different concentrations of treatment group, AST-IV group, BV group, AST-IV + BV group, Earle's balanced salt solution (EBSS) group, EBSS+AST-IV group, chloroquine (CQ, autophagy inhibitor) group, EBSS+CQ group, and CQ + BV group.

Cells in BV different concentrations of treatment group: A549 cells were treated by BV (No. 159752-10-0, Shenzhen Hualai Biotechnology Co., Ltd., Shenzhen, China) at different concentrations (0, 1, 5, 25, and 50 μmol/L) for 24 h. Cells in AST-IV different concentrations of treatment group: A549 cells were treated by AST-IV ($C_{41}H_{68}O_{14}$, purity 98%, No. ZL20130420HQ, Nanjing Zelang Medical Technology Co., Ltd., Nanjing, China) at different concentrations (0, 10, 20, 50, and 100 ng/ml) for 24 h. AST-IV group: A549 cells were treated by 50 ng/ml AST-IV for 24 h. BV group: A549 cells were treated by 25 μmol/L BV for 24 h. AST-IV + BV group: A549 cells were co-treated with BV (25 μmol/L) and AST-IV (50 ng/ml) for 24 h. EBSS group: A549 cells were treated with EBSS (No. SH30024.01, Shenzhen Zhongsheng Huanyu Biotechnology Co., Ltd, China). EBSS+AST-IV group: A549 cells were co-treated with EBSS and 50 ng/ml AST-IV. CQ group: A549 cells were treated with CQ (No.93-1825-100, Hangzhou Lianke Biotechnology Co., Ltd, China). EBSS+CQ group: A549 cells were co-treated with EBSS and CQ. CQ + BV group: A549 cells were co-treated with CQ and 25 μmol/L BV. Control group: A549 cells without any treatment were considered as control group.

2.2 | MTT assay

After A549 cells were treated with BV and AST-IV for 24 h, the effects of AST-IV and BV on the viability of A549 cells were observed. In brief, the cells (1×10^6/ml) were seeded into the 6-well plate. Twenty microliters of MTT solution (B7777, APExBIO, Houston, United States) was added to each well. A549 cells were incubated in the culture box for 4 h and the culture fluid in the well was then sucked out using a micropipette. One hundred and fifty microliters 0.5% DMSO (No. 67-68-5, Hubei Jusheng Technology Co., Ltd, Hubei, China) were added to each well and shaken gently for 10 min to fully dissolve the purple crystals. Finally, the OD value of each well was measured at 570 nm by a microplate reader (Infinite M200 PRO, Tecan Austria GmbH, Austria). All experiments were repeated three times and the average value was then calculated.

2.3 | Cell cycle

A549 cells (1×10^6/ml) were placed in a 12-well plate and were digested by trypsin (C0202, Beyotime Biotechnology, China) for 2 min. After that, the cells were fixed by 3 ml 70% ice ethanol for

48 h. All cell suspensions were centrifuged at 1000 × *g* at 4°C for 3 min and then discarded. The cells were washed three times by phosphate buffered saline (PBS). Four hundred microliters of 50 μg/ml propidium iodide (PI) (ST511, Beyotime Biotechnology, China) solution was used to stain the cells. In the end, the stained cells were analyzed by a flow cytometer (version 10.0, FACS CaliburTM, BD, Franklin Lakes, NJ, United States).

2.4 | Cell apoptosis

A549 cells (1×10^6/ml) were digested by trypsin for 2 min. Next, trypsin was discarded, 1 ml RPMI-1640 medium was added to cells and were repeatedly blown into a single cell fluid. All cell suspensions were transferred to 15 ml centrifugation tube and centrifuged at 1000 × *g* for 5 min at 4°C. Subsequently, the cells were resuspended in the solution containing 1 × Annexin binding buffer, and then 5 μl fluorescein isothiocyanate (FITC) Annexin V, 1 μl 100 μg/ml PI and the 300 μl1 × Annexin Binding Buffer were added to cell suspension. Ultimately, the stained cells were analyzed by flow cytometry.

2.5 | Western blotting

The cells were washed twice by cold PBS and the total protein was collected by IP cell lysis buffer (Shanghai Yili Biochemical Reagent Co., Ltd., China). Then the cells were put on ice for 20 min and centrifuged at 12,000 × *g* for 5 min at 4°C, with the supernatant being collected. The protein concentration was determined by bicinchoninic acid (BCA) assay (P0012S, Beyotime Biotechnology, China), which was calculated according to the standard curve. After that, the protein was boiled at 100°C for 5 min for denaturation, and the protein suspension was dissociated by 15% dodecyl sulfate sodium salt-polyacrylamide gel electrophoresis (SDS-PAGE). Next, the protein suspension was transferred to polyvinylidene fluoride (PVDF) membranes, which were sealed with 5% milk at room temperature for 1 h, and then incubated with appropriate dilutions of specific antibodies, including anti-sequestosome 1 (P62) (anti-SQSTM1, mouse, 1:1000, ab56416, Abcam), anti-microtubule associated protein 1 light chain 3 (anti-LC3B, rabbit, 1:1000, ab48394, Abcam), anti-phosphorylated-mTOR (anti-p-mTOR, rabbit, 1:1000, ab109268, Abcam), anti-B-cell lymphoma-2 (anti-Bcl-2, rabbit, 1:1000, ab59348, Abcam), anti-Bcl-2 associated × protein (anti-Bax, rabbit, 1:1000, ab32503, Abcam), anti-cleaved Caspase-3 (anti-C-Caspase-3, rabbit, 1:1000, ab2302, Abcam), anti-protein kinase B (anti-Akt, rabbit, 1:1000, #9272, CST), anti-phosphorylated-AKT (anti-p-Akt, rabbit, 1:1000, #9271, CST), anti-mammalian target of rapamycin (anti-mTOR, rabbit, 1:1000, ab2732, Abcam), and anti-glyceraldehyde-3-phosphate dehydrogenase (anti-GAPDH, mouse, 1:2000, ab8245, Abcam) at 4°C overnight. Then, the membranes were incubated with goat anti-mouse or goat anti-rabbit IgG (H + L) peroxidase-conjugated antibody (1:5000, No. 1034-05 or 4050-05, Southern Biotech, Birmingham, AL, United States) for 2 h and washed three times with PBS. The front and back of the membrane were in full contact with the developer. Finally, the membranes were scanned by an ultra-sensitive multifunctional imager (version 4.7, National Institutes of Health, United States).

2.6 | RNA isolation and quantitative reverse transcription-polymerase chain reaction

The total RNA was extracted from A549 cells using Trizol reagent (15596018, ThermoFisher Scientific, United States), while the concentration of RNA was measured by Nanodrop (Thermo Scientific™, San Diego, CA, United States) and diluted to 500 ng/μl. After the extraction of RNA, 1 μg RNA, 10 μmol/L dNTP mixture, and 0.5 μg oligo $(dT)_{15}$ primer were combined with water to form 20 μl mixed liquid in a microcentrifugation tube and reverse-transcribed into cDNA according to the instructions of the kit (Qingen, 218061, China). The reverse transcription conditions were as follows: at 42°C for 1 h, at 99°C for 5 min and at 16°C forever. The mRNA expression levels were determined by real-time polymerase chain reaction (PCR) using SYBR Green Real Time PCR kit (QIAGEN, 204054, China). Four microliters cDNA, 5 μl SYBR (Takara, codeDRR041A) and 1 μl primer were mixed together. PCR cycle was set as follows: 94°Capretreatment for 2 min, at 94°C for 30 s, at 63°C for 30 s, at 72°C for 1 min (35 cycles), chain extension at 72°C for 7 min and keep at 4°C. The products of quantitative reverse transcription-polymerase chain reaction (qRT-PCR) were analyzed by the ABI PRISM 7700 Sequence Detection System Instrument and software (MxPro QPCR Software version 4.1, SDS 1.9.1, PE Applied Biosystems, Inc., United States). All primer sequences were listed in Table 1.

TABLE 1 Primers used in real-time PCR analysis

Gene	Primer sequence	Species
P62	Forward: 5′-GCA CAC CAA GCT CGC ATT C-3′ reverse: 5′-ACC CGA AGT GTC CGT GTT TC-3′	Human
Beclin1	Forward: 5′-AACCAACGTCTTTAATGCA ACCTTC-3′ reverse: 5′-AGCAGCATTAATCTCATTC CATTCC-3′	Human
CTSB	Forward: 5′-GCTGTAATGGTGGCTATC CTGCT-3′ reverse: 5′-GTCTGCACCCTACATGGGA TTCA-3′	Human
CTSL	Forward: 5′-GGA TTATGCTTTCCAGT ATGTTCA-3′ reverse: 5′-CCTTCCCTGCTTAGGGATGTC-3′	Human
GAPDH	Forward: 5′-GGTGAAGGTCGGAGTCAAC G-3′ reverse: 5′-CAAAG TTGTCATGGATGTA CC-3′	Human

Abbreviations: CTSB, cathepsin B; CTSL, cathepsin L; p62, sequestosome 1.

2.7 | LysoTracker red staining

Lysotracker (LysoTracker Red C1046, Beyotime) staining was performed according to the manufacturer's instructions. In short, A549 cells were incubated in 6-well plates, and following the devised treatments, the cells were treated with 50 nM LysoTracker reagent for 5 min at 37°C. The fluorescence image was captured under fluorescence microscope.

2.8 | Statistical analysis

Prism 6 (version 6.01, Graph Pad Software, Inc., San Diego, CA, United States) was used for data analysis. The experimental data were shown as mean value ± SD ($M \pm SD$) and t test was used to compare the differences in the mean among continuous variables. Single factor analysis of variance was used to compare multiple groups. $p < .05$ was considered as statistically significant.

3 | RESULTS

3.1 | BV induced autophagy and blockage of autophagy promoted the apoptotic effect of BV

Initially, A549 cell was treated with BV at different concentrations (0, 1, 5, 25, and 50 μmol/L). As shown in Figure 1a, cell viability of A549 cell was inhibited by BV in a time-dependent manner ($p < .05$, $p < .01$, $p < .001$). Next, A549 cell was treated with AST-IV at different concentrations (0, 10, 20, 50, and 100 ng/ml) for 24 h, with the result indicating that the viability of cell was inhibited slightly ($p < .01$, Figure 1b). Furthermore, 50 ng/ml AST-IV combination with 25 μmol/L BV significantly inhibited the cell viability of A549 cells, which was statistically significant compared with the BV group, demonstrating the effect of AST-IV on cell viability after BV treatment ($p < .01$, Figure 1c). After the treatment of A549 cells by BV at different concentrations (0, 1, 5, and 25 μmol/L) for 24 h, the results showed that P62 expression was inhibited and Beclin1 expression was promoted in a dose-dependent manner ($p < .05$, $p < .01$, $p < .001$, Figure 1d). Moreover, the results of flow cytometry showed that the cell apoptosis was notably elevated in BV + CQ group than that in BV group ($p < .05$, $p < .01$, $p < .001$, Figure 1e,f).

3.2 | AST-IV inhibited autophagy by damaging lysosomal function and promoted the inhibitory effect of BV

Autophagy occurrence can affect the expression levels of p62, autophagy constituent proteins LC3-II/I and autophagy-related protein Beclin1. P62 is a selective substrate of autophagy involved in the recognition of ubiquitin-labeled substrates targeted for autophagy, and accumulation is observed when autophagy is repressed (Liu et al., 2016). Beclin1 induces the autophagy protein cascade (Xu & Qin, 2019).

To investigate the effect of AST-IV on autophagy of A549 cells, the expression levels of P62 and Beclin1 were detected by qRT-PCR, with the result demonstrating that after treating A549 cells by AST-IV at different concentrations for 24 h, the expression level of P62 was up-regulated dose-dependently, while that of Beclin1 was down-regulated dose-dependently ($p < .05$, $p < .01$, $p < .001$, Figure 2a). Therefore, AST-IV dose-dependently induced changes in the

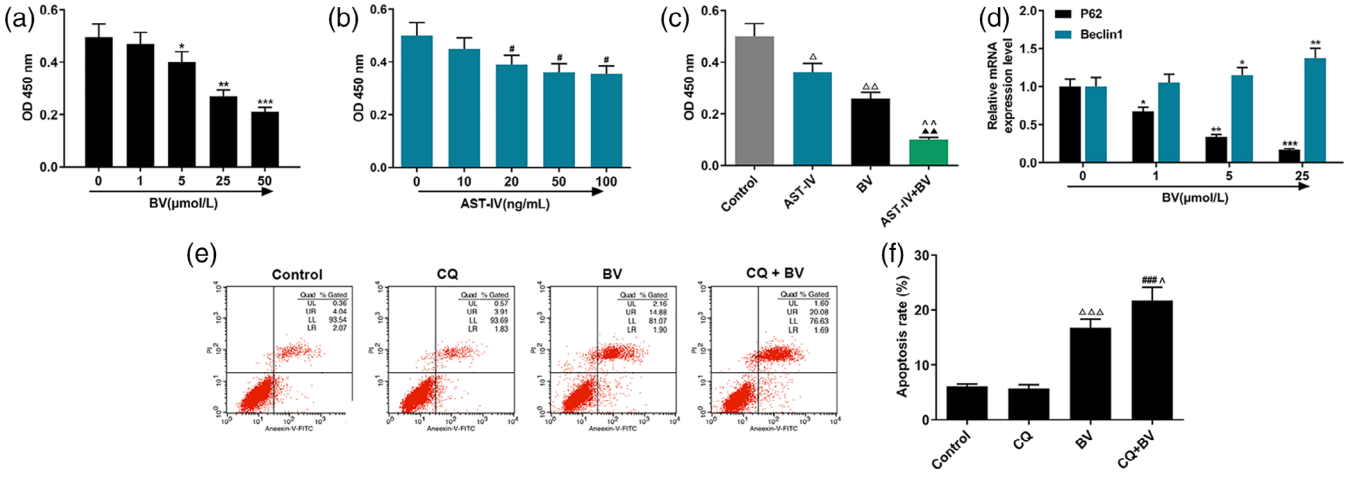

FIGURE 1 Bevacizumab (BV) induced autophagy and blockage of autophagy promoted the apoptotic effect of BV. (a) 3-(4,5-dimethyl-2-thiazolyl)-2,5-diphenyl-2-H-tetrazolium bromide (MTT) detection was performed on the cell viability of A549 cells treated by different concentrations (0, 1, 5, 25, and 50 μmol/L) of BV for 24 h ($^{*}p < .05$, vs. vehicle group. $^{\#}p < .05$, vs. 12 h. $^{\wedge}p < .05$, vs. 24 h). (b) The cell viabilities of A549 cells that treated by different concentrations (0, 10, 20, 50, and 100 ng/ml) of AST-IV for 24 h were detected by MTT. (c) MTT detection was performed on the cell viabilities of A549 cells treated by astragaloside-IV (AST-IV) + BV for 24 h ($^{\triangle\triangle}p < .01$, vs. control group. $^{\wedge\wedge}p < .01$, vs. AST-IV group. $^{\triangle\triangle}p < .01$, vs. BV group). (d) The expression levels of P62 and Beclin1 were detected in A549 cells by reverse transcription-polymerase chain reaction (qRT-PCR) treated with different concentrations (0, 1, 5, and 25 μmol/L) of BV for 24 h ($^{*}p < .05$, $^{**}p < .01$, $^{***}p < .001$, vs. 0 concentration BV-treatment group). (e) and (f) BV (25 μmol/L) and chloroquine (autophagy inhibitor) (CQ) were co-treated A549 cells, the cell apoptosis was determined by flow cytometry ($^{\triangle\triangle\triangle}p < .001$, vs. control group. $^{\wedge}p < .05$, vs. BV group. $^{\#\#\#}p < .001$, vs. CQ group)

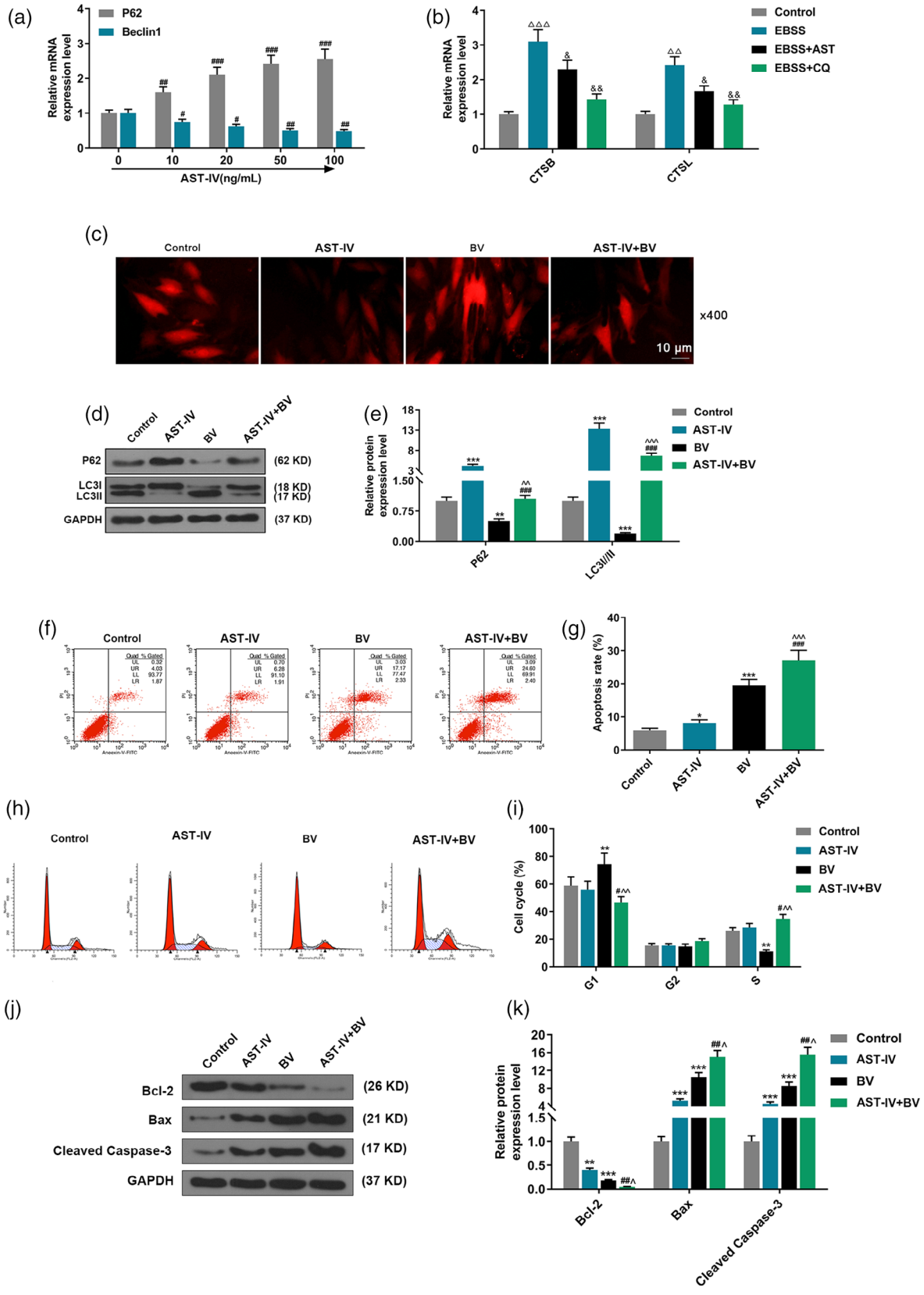

FIGURE 2 Legend on next page.

autophagy markers Beclin-1 and p62, indicating inhibition of autophagy. A previous paper demonstrated that the lysosomal function is controlled in the course of autophagy (Zhou et al., 2013). Thus, we attempted to investigate the effect of AST-IV on lysosomal function. One inimitable feature of lysosome is its highly acidic environment, which is a critical point in controlling the activity of cathepsin enzymatic and lysosomal function (Mindell, 2012). Lysosomal cathepsin B (CTSB) and cathepsin L (CTSL) are cysteine proteases physiologically associated with lysosomal protein degradation. In this study, A549 cells were treated with EBSS to affect its highly acidic environment. In accordance with the result, the expressions of lysosomal cathepsin B/L (CTSB/L) were increased in EBSS group compared to control group. Moreover, A549 cells were treated by EBSS and CQ or AST-IV, and the effects of AST-IV on the mRNA levels of CTSB and CTSL in A549 cells were evaluated. Consistent with the effect of CQ, AST-IV treatment reduced the mRNA levels of CTSB and CTSL in EBSS condition ($p < .05$, $p < .01$, $p < .001$, Figure 2b). Additionally, AST-IV treatment significantly decreased the fluorescence intensity of LysoTracker Red (Figure 2c). Compared with the AST-IV treatment group, the BV + AST-IV group exhibited upregulation of the fluorescence intensity of LysoTracker Red. Collectively, the data indicated that AST-IV suppressed autophagy by damaging the function of lysosome.

LC3 is a major effector of autophagy, and the conversion of LC3-I (free form of LC3) to LC3-II is an initiating step in autophagy activation in mammals (Kabeya et al., 2000). To investigate the effect of

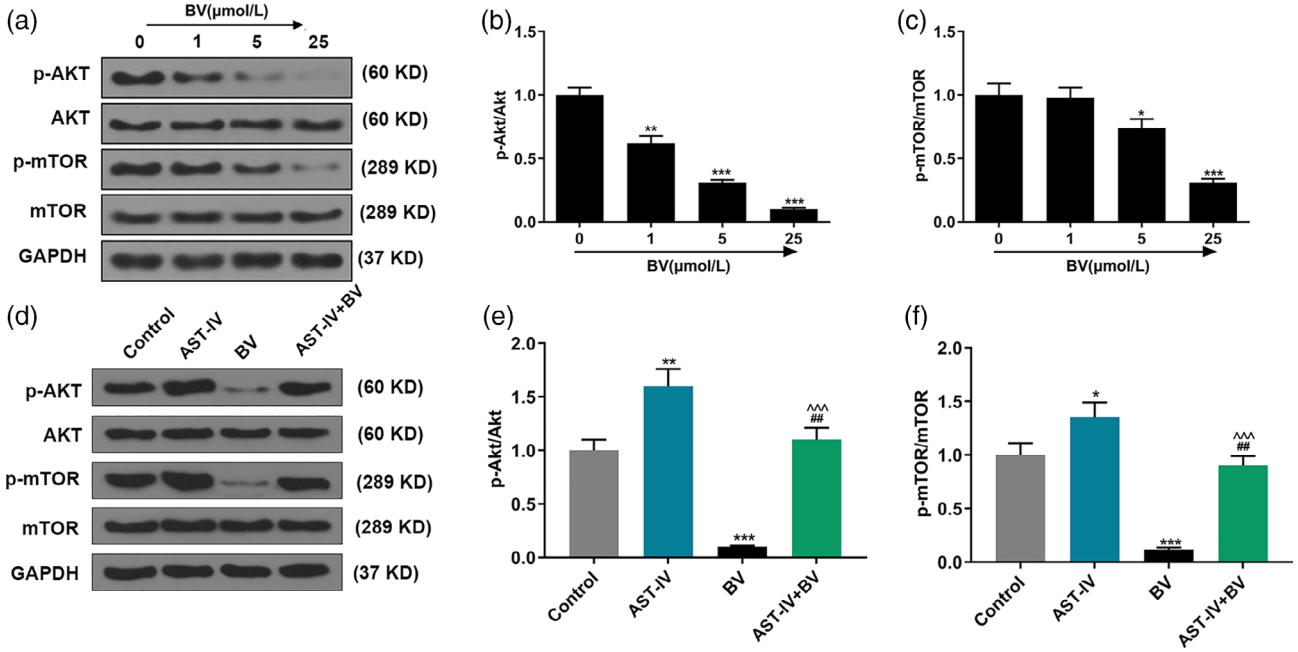

FIGURE 3 Astragaloside-IV (AST-IV) reversed the inhibitory effect of bevacizumab (BV) on Akt/mTOR pathway. (a), (b), and (c) The phosphorylation levels of p-Akt and p-mTOR were determined by western blotting in A549 cells treated by different concentrations (0, 1, 5, and 25 μmol/L) of BV for 24 h ($^{*}p < .01$, $^{**}p < .05$, $^{***}p < .001$, vs. 0 concentration BV-treatment group).(d), (e), and (f) The expression levels of p-AKT, AKT, p-mTOR, and mTOR in A549 cells that treated with BV and AST-IV were detected by western blotting ($^{*}p < .05$, $^{**}p < .01$, $^{***}p < .001$, vs. control group. $^{\#\#}p < .01$, vs. AST-IV group. $\hat{}p < .05$, vs. BV group)

FIGURE 2 Astragaloside-IV (AST-IV) inhibited autophagy by damaging lysosomal function and promoted the inhibitory effect of bevacizumab (BV). (a) Reverse transcription-polymerase chain reaction (qRT-PCR) detection was performed on the mRNA levels of P62 and Beclin1 in A549 cells treated by different concentrations of AST-IV for 24 h ($^{\#}p < .05$, $^{\#\#}p < .01$, $^{\#\#\#}p < .001$, vs. 0 concentration AST-IV-treatment group). (b) the mRNA levels of cathepsin B (CTSB) and cathepsin L (CTSL) were detected by qRT-PCR in A549 cells co-treated by AST-IV (50 ng/ml) and EBSS, or EBSS+CQ ($^{\triangle\triangle}p < .01$, vs. control group, $^{\&}p < .05$, $^{\&\&}p < .01$, vs. Earle's balanced salt solution [EBSS]).(c) LysoTracker red was used to specifically label intracellular lysosomes. Scale bar, 10 μm. (d) and (e) Western blotting was used to determine levels of P62 and LC3 I/LC3 II in A549 cell in the AST-IV (50 ng/ml) + BV (25 μmol/L) group and BV (25 μmol/L) group. (f) and (g) BV (25 μmol/L) and AST-IV (50 ng/ml) were co-treated A549 cell, and the cell apoptosis was examined by flow cytometry. (h) and (i) A549 cell in the AST-IV (50 ng/ml) + BV (25 μmol/L) group, AST-IV (50 ng/ml) group and BV (25 μmol/L) group was stained by propidium iodide (PI) and cell cycle distribution was analyzed by flow cytometry ($^{*}p < .05$, $^{**}p < .01$, $^{***}p < .001$ vs. control group. $^{\#}p < .05$, $^{\#\#}p < .01$ vs. AST-IV group. $\hat{}p < .05$ vs. BV group). (j) and (k) Western blotting was performed to analyze expression levels of B-cell lymphoma-2 (Bcl-2), Bcl-2 associated x protein (Bax), and Cleaved-cysteinyl aspartate specific proteinase-3 (Cleaved-caspase-3) in A549 cell treated by BV (25 μmol/L) for 24 h in the presence or absence of AST-IV (50 ng/ml) ($^{*}p < .01$, $^{**}p < .05$, $^{***}p < .001$ vs. control group. $^{\#}p < .05$, $^{\#\#}p < .01$ vs. AST-IV group. $\hat{}p < .05$ vs. BV group). MTT: 3-(4,5-dimethyl-2-thiazolyl)-2,5-diphenyl-2-H-tetrazolium bromide, SQSTM1 (P62): sequestosome 1

AST-IV on the sensitivity of A549 cells by enhancing BV, the expression levels of P62, LC3I, and LC3II were detected in A549 cell treated with AST-IV and BV. As shown in Figure 2d,e, in the light of the results, the levels of P62 and LC3I/LC3II in the AST-IV + BV group were significantly higher than that in BV group ($p < .05$, $p < .001$). Besides, the apoptosis of A549 cells was detected by flow cytometry, with the results revealing that the apoptosis rate in the AST-IV + BV group was markedly promoted than that in BV group ($p < .05$, $p < .01$, $p < .001$, Figure 2f,g). Moreover, an increase in the number of cells arrested at G0/G1 phase and a decrease of cells arrested at S phase in BV group were observed. AST-IV alone could not induce cell arrest in A549 cells, but AST-IV in combination with BV could induce S-stage arrest in A549 cells (Figure 2h,i). The levels of Bax and Cleaved-caspase-3 in AST-IV + BV group were significantly higher than those in the BV group, whereas the level of Bcl-2 in AST-IV + BV group was remarkably lower than that in BV group ($p < .05$, Figure 2j,k).

3.3 | AST-IV reversed the inhibitory effect of BV-induced inhibiting on Akt/mTOR pathway

Furthermore, the results of western blotting indicated that the phosphorylation levels of AKT and mTOR were effectively down-regulated in a dose-dependent manner ($p < .05$, $p < .01$, $p < .001$, Figure 3a–c). The phosphorylation levels of AKT and mTOR were effectively down-regulated in A549 cells by treating with BV, but were notably up-regulated in A549 cells co-treated with AST-IV and BV ($p < .05$, $p < .01$, $p < .001$, Figure 3d–f).

4 | DISCUSSION

BV leads to ischemia and hypoxia of tumor cells by blocking viability of tumor vascular endothelial growth factor so as to affect tumor growth (Lin et al., 2018). Currently, BV has been widely used in treating a variety of cancers with certain satisfactory results (Yang et al., 2017). In this study, we found that BV dose-dependently inhibited viabilities of A549 cells, which was similar to research results obtained by Zhao et al. (2018) in exploring the effect of BV on the proliferation of colorectal cancer cells.

Traditional Chinese medicine is gradually applied to treating tumor, and AST-IV has achieved satisfactory results in anti-tumor treatment (Xie et al., 2016). In this study, we investigated the effect of AST-IV on the cell viability of A549 cells, and figured out that the viability was inhibited in a concentration-dependent manner. In order to further explore the effect of AST-IV on A549 cells, A549 cells were treated by AST-IV in combination with BV, and it was found that the combined treatment as such significantly inhibited cell viability compared with BV alone. AST-IV has been confirmed to exert the inhibitory effect on tumor angiogenesis (Zhang et al., 2017). Thus, we speculated that AST-IV alone has no obvious cytotoxic effect on A549.

Cell proliferation is achieved by cell cycle. Currently, a regulatory site affecting cell cycle exists between G1 phase and S phase or between G2 phase and M phase (Du et al., 2017; Li et al., 2018). Once a cell passes through the regulatory site, drugs can no longer prevent the cell from entering or transforming into M phase through S phase (Li et al., 2018). In this study, flow cytometry was used to observe the effects of BV and AST-IV on cell cycle. The results showed that after treating A549 cells by BV, an increase in the number of cells arrested at G0/G1 phase and a decrease in those arrested at S phase were observed. AST-IV acting alone on A549 cells might not induce cell arrest. However, AST-IV and BV in combination induce cell arrest at S phase, possibly owing to the fact that the two drugs inhibited the proliferation of tumor cells via blocking the signal transduction pathways at different periods, and the time-phase distribution of tumor cells could affect the cell cycle.

Apoptotic disorder is considered as one of the main factors contributing to uncontrolled tumor growth (Palladino et al., 2016). Our results demonstrated that AST-IV could enhance the effect of BV on promoting cell apoptosis. In addition, Bcl-2 is a key regulator of the intrinsic or mitochondrial pathway for apoptosis. Gao et al. (2016) proposed that the expression of Bcl-2 was decreased as apoptosis accelerated. Increased Bax and Cleaved-caspase-3 protein expressions and decreased Bcl-2 protein expression indicate the accelerated cell apoptosis (Dolka et al., 2016; Gao et al., 2016). In this study, changes in Bax, Bcl-2, and Cleaved-caspase-3 levels showed that the combination of AST-IV and BV can promote apoptosis compared to BV alone, suggesting that the combination of AST-IV and BV induced apoptosis by regulating the expressions of Bcl-2, Bax, and c-cleaved 3 proteins in the cells.

Autophagy, which has become an important factor for developing drug resistance in advanced tumor cells, enhances the ability of tumor cells to survive in adverse environments (Song et al., 2017). The crosstalk of proteins modulating both autophagy and apoptosis exists (Liu et al., 2017). Based on an existing research, autophagy can affect the sensitivity of tumor cells to chemotherapy drugs (Domagala et al., 2018). We found that AST-IV could promote the P62 expression and inhibit that of Beclin1. Besides, similar to the effect of CQ, AST-IV also inhibited CTSB and CTSL expressions, suggesting that AST-IV had a certain inhibitory effect on autophagy by damaging lysosomal function.

P62 and LC3 were reported to be highly expressed in many types of human malignancies and are associated with prognosis in patients who received anti-tumor treatment (Schlafli et al., 2016). Thus, the expressions of LC3 and P62 were detected in BV-treated A549 cells. In accordance with the results, BV inhibited expression levels of P62 and LC3I/LC3II, indicating that BV can promote autophagy, which was consistent with the results posed by Liang et al. (2015). However, AST-IV could reverse the effect of BV on autophagy related proteins. In addition, Akt/mTOR signal plays a key role in the negative regulation of autophagy (Mathews & Appel, 2016). It has been reported that the activation of mTOR regulates protein synthesis by phosphorylation of downstream p70S6K (Lian et al., 2018; Somers et al., 2013). Nazim et al. (2017) reported

inhibition of Akt/mTOR promoted cell death in human lung adenocarcinoma cells through activating autophagy flux. Xu et al. (2021) also demonstrated hippo pathway effector YAP could induce activation of Akt/mTOR signaling pathway to regulate cell proliferation via autophagy in lung adenocarcinomas. Increasing evidence has also showed the regulatory association between Akt/mTOR signaling pathway and autophagy in lung adenocarcinomas (Chen et al., 2017; Huo et al., 2016; Jian et al., 2019; Wang et al., 2018). This study confirmed that BV could induce the AKT/mTOR pathway in lung adenocarcinoma cells, which may involve with the regulation of autophagy in lung adenocarcinomas cells, whereas AST-IV could reverse the effect of BV on Akt/mTOR signal pathway. Thus, we speculated that AST-IV enhanced the effects of BV on promoting apoptosis of A549 cells by inhibiting autophagy.

5 | CONCLUSION

In conclusion, AST-IV combined with BV inhibited cell proliferation and promoted apoptosis. In addition, AST-IV might promote the sensitivity of A549 cell to BV through regulation of autophagy protein. However, there are some limitations in this study. For example, the autophagic mechanism of the two-drug combination treatment for lung adenocarcinoma cell might not be comprehensive, as only in vitro experiments were carried out. Thus, further in-depth investigation is required to prove that AST-IV enhances the sensitivity of lung adenocarcinoma cell to BV via autophagic pathway.

CONFLICT OF INTEREST

The authors declare no conflicts of interest.

DATA AVAILABILITY STATEMENT

The analysed data sets generated during the study are available from the corresponding author on reasonable request.

ORCID

Renzhong Cai https://orcid.org/0000-0001-5564-3079

REFERENCES

Bade, B. C., & Dela Cruz, C. S. (2020). Lung cancer 2020: Epidemiology, etiology, and prevention. *Clinics in Chest Medicine*, *41*(1), 1–24.

Cao, Z., Zhang, H., Cai, X., Fang, W., Chai, D., Wen, Y., Chen, H., Chu, F., & Zhang, Y. (2017). Luteolin promotes cell apoptosis by inducing autophagy in hepatocellular carcinoma. *Cellular Physiology and Biochemistry: International Journal of Experimental Cellular Physiology, Biochemistry, and Pharmacology*, *43*(5), 1803–1812.

Chen, J., Yuan, J., Zhou, L., Zhu, M., Shi, Z., Song, J., Xu, Q., Yin, G., Lv, Y., Luo, Y., Jia, X., & Feng, L. (2017). Regulation of different components from *Ophiopogon japonicus* on autophagy in human lung adenocarcinoma A549Cells through PI3K/Akt/mTOR signaling pathway. *Biomedicine & Pharmacotherapy*, *87*, 118–126.

Chen, Y., Sun, Y., Zhao, W., Ma, Y., Yan, Z., & Nie, X. (2020). Elevated SRC3 expression predicts pemetrexed resistance in lung adenocarcinoma. *Biomedicine & Pharmacotherapy*, *125*, 109958.

Dolka, I., Krol, M., & Sapierzynski, R. (2016). Evaluation of apoptosis-associated protein (Bcl-2, Bax, cleaved caspase-3 and p53) expression in canine mammary tumors: An immunohistochemical and prognostic study. *Research in Veterinary Science*, *105*, 124–133.

Domagala, A., Stachura, J., Gabrysiak, M., Muchowicz, A., Zagozdzon, R., Golab, J., & Firczuk, M. (2018). Inhibition of autophagy sensitizes cancer cells to photofrin-based photodynamic therapy. *BMC Cancer*, *18*(1), 210.

Du, S., Lu, L., Miao, Y., Jin, W., Li, C., Xin, Y., & Xuan, S. (2017). E167K polymorphism of TM6SF2 gene affects cell cycle of hepatocellular carcinoma cell HEPA 1-6. *Lipids in Health and Disease*, *16*(1), 76.

Gao, M., Li, Y., Ji, X., Xue, X., Chen, L., Feng, G., Zhang, H., Wang, H., Shah, W., Hou, Z., & Kong, Y. (2016). Disturbance of Bcl-2, Bax, Caspase-3, Ki-67 and C-myc expression in acute and subchronic exposure to benzo(a)pyrene in cervix. *Acta Histochemica*, *118*(2), 63–73.

He, C. S., Liu, Y. C., Xu, Z. P., Dai, P. C., Chen, X. W., & Jin, D. H. (2016). Astragaloside IV enhances cisplatin chemosensitivity in non-small cell lung cancer cells through inhibition of B7-H3. *Cellular Physiology and Biochemistry: International Journal of Experimental Cellular Physiology, Biochemistry, and Pharmacology*, *40*(5), 1221–1229.

Huang, F., Wang, B. R., & Wang, Y. G. (2018). Role of autophagy in tumorigenesis, metastasis, targeted therapy and drug resistance of hepatocellular carcinoma. *World Journal of Gastroenterology*, *24*(41), 4643–4651.

Huang, H., Song, J., Liu, Z., Pan, L., & Xu, G. (2018). Autophagy activation promotes bevacizumab resistance in glioblastoma by suppressing Akt/mTOR signaling pathway. *Oncology Letters*, *15*(2), 1487–1494.

Huo, R., Wang, L., Liu, P., Zhao, Y., Zhang, C., Bai, B., Liu, X., Shi, C., Wei, S., & Zhang, H. (2016). Cabazitaxel-induced autophagy via the PI3K/Akt/mTOR pathway contributes to A549 cell death. *Molecular Medicine Reports*, *14*(4), 3013–3020.

Jian, M., Yunjia, Z., Zhiying, D., Yanduo, J., & Guocheng, J. (2019). Interleukin 7 receptor activates PI3K/Akt/mTOR signaling pathway via down-regulation of Beclin-1 in lung cancer. *Molecular Carcinogenesis*, *58*(3), 358–365.

Jiang, Y., Han, Z., Wang, Y., & Hao, W. (2018). Depletion of SIRT7 sensitizes human non-small cell lung cancer cells to gemcitabine therapy by inhibiting autophagy. *Biochemical and Biophysical Research Communications*, *506*(1), 266–271.

Kabeya, Y., Mizushima, N., Ueno, T., Yamamoto, A., Kirisako, T., Noda, T., Kominami, E., Ohsumi, Y., & Yoshimori, T. (2000). LC3, a mammalian homologue of yeast Apg8p, is localized in autophagosome membranes after processing. *The EMBO Journal*, *19*(21), 5720–5728.

Levy, J. M. M., Towers, C. G., & Thorburn, A. (2017). Targeting autophagy in cancer. *Nature Reviews Cancer*, *17*(9), 528–542.

Li, W., Liu, J., Fu, W., Zheng, X., Ren, L., Liu, S., Wang, J., Ji, T., & Du, G. (2018). 3-O-acetyl-11-keto-beta-boswellic acid exerts anti-tumor effects in glioblastoma by arresting cell cycle at G2/M phase. *Journal of Experimental & Clinical Cancer Research: CR*, *37*(1), 132.

Li, Y. J., Lei, Y. H., Yao, N., Wang, C. R., Hu, N., Ye, W. C., Zhang, D. M., & Chen, Z. S. (2017). Autophagy and multidrug resistance in cancer. *Chinese Journal of Cancer*, *36*(1), 52.

Lian, X., Gu, J., Gao, B., Li, Y., Damodaran, C., Wei, W., Fu, Y., & Cai, L. (2018). Fenofibrate inhibits mTOR-p70S6K signaling and simultaneously induces cell death in human prostate cancer cells. *Biochemical and Biophysical Research Communications*, *496*(1), 70–75.

Liang, J., Piao, Y., Henry, V., Tiao, N., & de Groot, J. F. (2015). Interferon-regulatory factor-1 (IRF1) regulates bevacizumab induced autophagy. *Oncotarget*, *6*(31), 31479–31492.

Lin, H. Y., Kuo, W. T., & Hsu, C. W. (2018). Laparoscopic repair of bevacizumab-induced vesicovaginal fistula in metastatic colon cancer—A video vignette. *Colorectal Disease: The Official Journal of the Association of Coloproctology of Great Britain and Ireland*, *21*(1), 123.

Liu, G., Pei, F., Yang, F., Li, L., Amin, A. D., Liu, S., Buchan, J. R., & Cho, W. C. (2017). Role of autophagy and apoptosis in non-small-cell lung cancer. *International Journal of Molecular Sciences*, *18*(2), 367.

Liu, W. J., Ye, L., Huang, W. F., Guo, L. J., Xu, Z. G., Wu, H. L., Yang, C., & Liu, H. F. (2016). p62 links the autophagy pathway and the

ubiqutin-proteasome system upon ubiquitinated protein degradation. *Cellular & Molecular Biology Letters*, *21*, 29.

Müller-Greven, G., Carlin, C. R., Burgett, M. E., Ahluwalia, M. S., Lauko, A., Nowacki, A. S., Herting, C. J., Qadan, M. A., Bredel, M., Toms, S. A., Lathia, J. D., Hambardzumyan, D., Sarkaria, J. N., Hamerlik, P., & Gladson, C. L. (2017). Macropinocytosis of bevacizumab by glioblastoma cells in the perivascular niche affects their survival. *Clinical Cancer Research: An Official Journal of the American Association for Cancer Research*, *23*(22), 7059–7071.

Ma, M., She, Y., Ren, Y., Dai, C., Zhang, L., Xie, H., Wu, C., Yang, M., Xie, D., & Chen, C. (2018). Micropapillary or solid pattern predicts recurrence free survival benefit from adjuvant chemotherapy in patients with stage IB lung adenocarcinoma. *Journal of Thoracic Disease*, *10*(9), 5384–5393.

Mathews, E. S., & Appel, B. (2016). Cholesterol biosynthesis supports myelin gene expression and axon ensheathment through modulation of P13K/Akt/mTor signaling. *The Journal of Neuroscience: The Official Journal of the Society for Neuroscience*, *36*(29), 7628–7639.

Meher, J. G., Dixit, S., Pathan, D. K., Singh, Y., Chandasana, H., Pawar, V. K., Sharma, M., Bhatta, R. S., Konwar, R., Kesharwani, P., & Chourasia, M. K. (2018). Paclitaxel-loaded TPGS enriched self-emulsifying carrier causes apoptosis by modulating survivin expression and inhibits tumour growth in syngeneic mammary tumours. *Artificial Cells, Nanomedicine, and Biotechnology*, *46*(sup3), S344–S358.

Mindell, J. A. (2012). Lysosomal acidification mechanisms. *Annual Review of Physiology*, *74*, 69–86.

Nazim, U. M., Moon, J. H., Lee, Y. J., Seol, J. W., Kim, Y. J., & Park, S. Y. (2017). Glipizide sensitizes lung cancer cells to TRAIL-induced apoptosis via Akt/mTOR/autophagy pathways. *Oncotarget*, *8*(59), 100021–100033.

Palladino, G., Notarangelo, T., Pannone, G., Piscazzi, A., Lamacchia, O., Sisinni, L., Spagnoletti, G., Toti, P., Santoro, A., Storto, G., Bufo, P., Cignarelli, M., Esposito, F., & Landriscina, M. (2016). TRAP1 regulates cell cycle and apoptosis in thyroid carcinoma cells. *Endocrine-Related Cancer*, *23*(9), 699–709.

Ramezani, S., Vousooghi, N., Joghataei, M. T., & Chabok, S. Y. (2019). The role of kinase signaling in resistance to bevacizumab therapy for glioblastoma multiforme. *Cancer Biotherapy & Radiopharmaceuticals*, *34*(6), 345–354.

Rossi, L., Verrico, M., Zaccarelli, E., Papa, A., Colonna, M., Strudel, M., Vici, P., Bianco, V., & Tomao, F. (2017). Bevacizumab in ovarian cancer: A critical review of phase III studies. *Oncotarget*, *8*(7), 12389–12405.

Schlafli, A. M., Adams, O., Galvan, J. A., Gugger, M., Savic, S., Bubendorf, L., Schmid, R. A., Becker, K. F., Tschan, M. P., Langer, R., & Berezowska, S. (2016). Prognostic value of the autophagy markers LC3 and p62/SQSTM1 in early-stage non-small cell lung cancer. *Oncotarget*, *7*(26), 39544–39555.

Shan, Y., Gao, Y., Jin, W., Fan, M., Wang, Y., Gu, Y., Shan, C., Sun, L., Li, X., Yu, B., Luo, Q., & Xu, Q. (2019). Targeting HIBCH to reprogram valine metabolism for the treatment of colorectal cancer. *Cell Death & Disease*, *10*(8), 618.

Somers, J., Poyry, T., & Willis, A. E. (2013). A perspective on mammalian upstream open reading frame function. *The International Journal of Biochemistry & Cell Biology*, *45*(8), 1690–1700.

Song, P., Jiang, B., Liu, Z., Ding, J., Liu, S., & Guan, W. (2017). A three-lncRNA expression signature associated with the prognosis of gastric cancer patients. *Cancer Medicine*, *6*(6), 1154–1164.

Tamura, R., Tanaka, T., Miyake, K., Yoshida, K., & Sasaki, H. (2017). Bevacizumab for malignant gliomas: Current indications, mechanisms of action and resistance, and markers of response. *Brain Tumor Pathology*, *34*(2), 62–77.

Tian, W., Hao, S., Gao, B., Jiang, Y., Zhang, X., Zhang, S., Guo, L., Zhao, J., Zhang, G., Chen, Y., Li, Z., & Luo, D. (2018). Lobaplatin inhibits breast cancer progression, cell proliferation while it induces cell apoptosis by downregulating MTDH expression. *Drug Design, Development and Therapy*, *12*, 3563–3571.

Toyokawa, G., Yamada, Y., Tagawa, T., Kozuma, Y., Matsubara, T., Haratake, N., Takamori, S., Akamine, T., Oda, Y., & Maehara, Y. (2018). Significance of spread through air spaces in resected pathological stage I lung adenocarcinoma. *The Annals of Thoracic Surgery*, *105*(6), 1655–1663.

Wang, L., Tan, Y., Gao, L., Lei, J., Chen, C., & Shi, Y. (2020). Effect of astragaloside on diaphragm cell apoptosis in chronic obstructive pulmonary disease. *Food Science & Nutrition*, *8*(12), 6357–6366.

Wang, Q., Guo, Y., Jiang, S., Dong, M., Kuerban, K., Li, J., Feng, M., Chen, Y., & Ye, L. (2018). A hybrid of coumarin and phenylsulfonylfuroxan induces caspase-dependent apoptosis and cytoprotective autophagy in lung adenocarcinoma cells. *Phytomedicine: International Journal of Phytotherapy and Phytopharmacology*, *39*, 160–167.

Wu, H. B., Yang, S., Weng, H. Y., Chen, Q., Zhao, X. L., Fu, W. J., Niu, Q., Ping, Y. F., Wang, J. M., Zhang, X., Yao, X. H., & Bian, X. W. (2017). Autophagy-induced KDR/VEGFR-2 activation promotes the formation of vasculogenic mimicry by glioma stem cells. *Autophagy*, *13*(9), 1528–1542.

Xie, T., Li, Y., Li, S. L., & Luo, H. F. (2016). Astragaloside IV enhances cisplatin chemosensitivity in human colorectal cancer via regulating NOTCH3. *Oncology Research*, *24*(6), 447–453.

Xu, H. D., & Qin, Z. H. (2019). Beclin 1, Bcl-2 and autophagy. *Advances in Experimental Medicine and Biology*, *1206*, 109–126.

Xu, W., Zhang, M., Li, Y., Wang, Y., Wang, K., Chen, Q., Zhang, R., Song, W., Huang, Q., Zhao, W., & Wu, J. (2021). YAP manipulates proliferation via PTEN/AKT/mTOR-mediated autophagy in lung adenocarcinomas. *Cancer Cell International*, *21*(1), 30.

Yang, R. F., Yu, B., Zhang, R. Q., Wang, X. H., Li, C., Wang, P., Zhang, Y., Han, B., Gao, X. X., Zhang, L., & Jiang, Z. M. (2017). Bevacizumab and gefitinib enhanced whole-brain radiation therapy for brain metastases due to non-small-cell lung cancer. *Brazilian Journal of Medical and Biological Research*, *51*(1), e6073.

Zhang, S., Tang, D., Zang, W., Yin, G., Dai, J., Sun, Y. U., Yang, Z., Hoffman, R. M., & Guo, X. (2017). Synergistic inhibitory effect of traditional Chinese medicine astragaloside IV and curcumin on tumor growth and angiogenesis in an orthotopic nude-mouse model of human hepatocellular carcinoma. *Anticancer Research*, *37*(2), 465–473.

Zhao, Z., Xia, G., Li, N., Su, R., Chen, X., & Zhong, L. (2018). Autophagy inhibition promotes bevacizumab-induced apoptosis and proliferation inhibition in colorectal cancer cells. *Journal of Cancer*, *9*(18), 3407–3416.

Zheng, Y., Dai, Y., Liu, W., Wang, N., Cai, Y., Wang, S., Zhang, F., Liu, P., Chen, Q., & Wang, Z. (2018). Astragaloside IV enhances taxol chemosensitivity of breast cancer via caveolin-1-targeting oxidant damage. *Journal of Cellular Physiology*, *234*(4), 4277–4290.

Zhou, J., Tan, S. H., Nicolas, V., Bauvy, C., Yang, N. D., Zhang, J., Xue, Y., Codogno, P., & Shen, H. M. (2013). Activation of lysosomal function in the course of autophagy via mTORC1 suppression and autophagosome-lysosome fusion. *Cell Research*, *23*(4), 508–523.

How to cite this article: Li, L., Li, G., Chen, M., & Cai, R. (2021). Astragaloside IV enhances the sensibility of lung adenocarcinoma cells to bevacizumab by inhibiting autophagy. *Drug Development Research*, 1–9. https://doi.org/10.1002/ddr.21878